Localized molecular orbitals for calculation and analysis of vibrational Raman optical activity

Luber, Sandra

Abstract: We present a novel method for the calculation of vibrational Raman optical activity (ROA) spectra based on localized molecular orbitals. This allows to split total ROA intensities into contributions of subsets, which can be chosen flexibly depending on the question of interest. It provides an appealing way to gain deeper insight into the factors influencing chirality and associated bands observed in the spectrum. As example, the ROA spectrum of a tryptophan model system, in particular the band arising from its W3 vibration, has been investigated.

DOI: https://doi.org/10.1039/c8cp05880f

Localized molecular orbitals for calculation and analysis of vibrational Raman optical activity

Sandra Luber[1]

Department of Chemistry, University of Zurich, Winterthurerstrasse 190,

8057 Zurich, Switzerland

[1]E-Mail: sandra.luber@chem.uzh.ch

Abstract

We present a novel method for the calculation of vibrational Raman optical activity (ROA) spectra based on localized molecular orbitals. This allows to split total ROA intensities into contributions of subsets, which can be chosen flexibly depending on the question of interest. It provides an appealing way to gain deeper insight into the factors influencing chirality and associated bands observed in the spectrum. As example, the ROA spectrum of a tryptophan model system, in particular the band arising from its W3 vibration, has been investigated.

1 Introduction

Localized molecular orbitals (LMOs) have been an active topic of research for decades and proven to be very useful for efficient computation and analysis of compounds. They can provide a comprehensive interpretation of the electronic structure and an intuitive understanding of the nature of bonding and associated properties. Besides that, localized molecular orbitals have been an important ingredient for reducing the computational effort of, e.g., correlated wave function-based methods (for reviews, see Refs. [1–3]). Whereas LMOs have a long-standing history in quantum chemistry, this approach has been extended to periodic systems later such as the concept of maximally localized Wannier functions [4, 5] by Marzari and Vanderbilt in 1997.

Among the different applications of LMOs, elucidation of spectroscopic signatures has been attractive, e.g. in order to study how they arise and what parts of a molecule determine their behaviour. For chiral compounds, vibrational spectroscopy has been an essential tool to investigate their structure and dynamics. For instance, the chiral variant of Infrared spectroscopy, vibrational circular dichroism, has been regularly applied to the study of molecules [6, 7]. The chiral variant of Raman spectroscopy, vibrational Raman optical activity (ROA) [8–11], has become more popular rather lately. Recent progress in this area encompasses, for example, the measurement of paramagnetic ROA [12], spectrometer for the deep-ultraviolet region [13], and first ROA spectra of chiral ionic liquids using a combined experimental/computational approach [14]. Whereas proteins [15–22], carbohydrates [23–25], and polymers [26, 27] have been studied more frequently (see reviews in Refs. [28–32]), the field of chiral metal complexes is a relatively new field of research [22, 33–36]. A review about ROA of coordination compounds and solids can be found in Ref. [37]. Computational advances based on first principles have included molecules-in-molecules fragment approaches [38], density fitting with massive parallel calculations [33], coupled cluster [39], and Cartesian transfer [40] techniques as well as

analytic calculation of ROA intensities [30, 41, 42], mode-selective ("intensity-tracking") methods [24, 43, 44], ROA spectra from *ab initio* molecular dynamics [45], and extension to resonance with electronically excited states [34, 46–48].

In order to gain insight into the contributions of certain atoms or group of atoms to ROA signals, analysis employing group coupling matrices has been suggested by Hug [49]. This relies on partition of the derivatives of the ROA property tensors with respect to nuclear coordinates of chosen atoms according to their contributions to the normal mode of interest. Localization of normal modes for the investigation of larger systems has been reported as well [15]. Complementary to that, the use of LMOs would allow another direction in analysis of ROA bands since they make an *a priori* partitiooning of the contributions of subgroups possible for the ROA property tensors themselves. Thus, a fragmentation at the level of the derivatives with respect to nuclear coordinates/normal coordinates is not required. Such an attractive computational approach using LMOs has been presented for VCD already in the early days of its development, namely by Nafie and Walnut in 1977 [50, 51]. In contrast to that, LMO-based ROA calculations have, to the best of our knowledge, not been reported although the idea had been proposed by Nafie and Freedman in 1981 [52].

In this manuscript, we present a computational approach for the calculation of ROA spectra based on LMOs. We use density functional perturbation theory (DFPT) to efficiently calculate the ROA property tensors. Moreover, we describe first LMO-based calculations with tryptophan as example, which shows an easily detectable optical response in ROA spectra and has been subject of previous investigations [53–57]. In particular, the intense W3 vibration is further examined based on fragmentation of the molecule into subgroups and their contributions to the overall ROA intensity. Besides potential future applications of this approach for accurate calculation of challenging systems such as liquids and larger compounds, the described methodology paves the way for novel insight into mechanisms

determining ROA intensities.

The manuscript is structured as follows: First, the computational approach and underlying theory are given in Section 2 followed by description of the computational methodology in Section 3. Afterwards, its application to tryptophan is presented as well as a detailed analysis of the W3 vibration in Section 4. A conclusion and outlook can be found in Section 5.

2 Theoretical background

ROA intensities for the backscattering experimental set-up are given by [58, 59]

$$(I^R - I^L)(180^\circ) \propto \beta(\mathbf{G}')^2 + \frac{1}{3}\beta(\mathbf{A})^2 \tag{1}$$

using the far from resonance approximation, i.e. no resonance with an electronic transition (for (electronic) resonance ROA, see Refs. [34, 46, 47] for first calculations in this field). We use the static limit $\omega_L \to 0$ (with ω_L being the angular frequency of the incident light), and the anisotropic ROA invariants are obtained for non-metallic systems as [60]

$$\beta(\mathbf{G}')^2 = \frac{1}{2}(3\alpha_{\alpha\beta}G'_{\alpha\beta} - \alpha_{\alpha\alpha}G'_{\beta\beta}) \tag{2}$$

$$\beta(\mathbf{A})^2 = \frac{1}{2}\alpha_{\alpha\beta}\epsilon_{\alpha\gamma\delta}A_{\gamma,\delta\beta} \tag{3}$$

where summation over repeated Greek indices is implied. $\epsilon_{\alpha\gamma\delta}$ is the $\alpha\gamma\delta$ (Greek indices indicate the Cartesian x/y/z directions) component of the (Levi-Civita) third-rank anti-symmetric unit tensor. The $\alpha\beta$ components of the electric-dipole–electric-dipole tensor $\boldsymbol{\alpha}$ and the electric-dipole–magnetic-dipole tensor $\mathbf{G}'$ are given as $\alpha_{\alpha\beta}$ and $G'_{\alpha\beta}$, respectively, and the $\gamma\delta\beta$ component of the electric-dipole–electric-quadrupole polarizability tensor $\mathbf{A}$ as $A_{\gamma,\delta\beta}$. In the double-harmonic approximation [61], the ROA intensities are evaluated using derivatives of the ROA tensor components with respect to normal coordinates. In

molecular dynamics calculations, the ROA intensities can be obtained via time correlation functions of tensor elements [45].

In order to obtain a local analysis in terms of LMOs, Kohn–Sham orbitals $\{|\psi_i\rangle\}$ are transformed to LMOs $\{|\tilde{\psi}_l\rangle\}$ via

$$|\tilde{\psi}_l\rangle = \sum_i V_{li}|\psi_i\rangle \tag{4}$$

with the transformation matrix $\mathbf{V}$. Wannier centers can be calculated for a periodic cubic unit cell with length L (using the Γ point of the Brillouin zone only) via the maximally localized Wannier function approach [4, 5] as

$$a_{\alpha,l}^{\mathrm{WC}} = -\frac{L}{2\pi}\mathrm{Im}\ln s_{\alpha,l} = -\frac{L}{2\pi}\mathrm{Im}\ln\left\langle\tilde{\psi}_l\left|\exp\left\{-\mathrm{i}\frac{2\pi}{L}r_\alpha\right\}\right|\tilde{\psi}_l\right\rangle. \tag{5}$$

r_α is the α component of the position operator. For non-periodic systems, the center of charge (c_{charge}) is obtained as

$$\mathbf{a}_l^{\mathrm{cc}} = \left\langle\tilde{\psi}_l\left|\mathbf{r}\right|\tilde{\psi}_l\right\rangle. \tag{6}$$

We use the localization criterion of minimizing the sum of the quadratic spreads (Foster–Boys) criterion in the non-periodic calculations [62–64], which corresponds to the Marzari–Vanderbilt criterion for periodic systems [5, 64] (see also the derivation of local electric dipole moments from periodic subsystem DFT in Ref. [65]).

We have recently described the efficient calculation of Raman [66] and ROA property tensors via DFPT [45]. In order to obtain the ROA tensors in terms of LMOs, the DFPT procedure has been modified accordingly. The unperturbed KS orbitals are localized via the unitary transformation as described in Eq. 4 and we assume that this transformation is sufficient for an analogous localization of the perturbed KS orbitals as well (we have not applied a transformation matrix beyond zeroth order [67, 68]).

Choosing a subset U and setting the gauge origin used for the calculation of the ROA

polarizability tensors to the positions of charge centers $\{\mathbf{a}_s^{\mathrm{cc}}\}$ leads to

$$\begin{aligned}
\alpha_{\alpha\beta}^{U} &= f_{\mathrm{occ}}\frac{2}{\hbar}\sum_{\substack{s\neq t\\ s\in U}}\frac{\langle\tilde{\psi}_s^{(0)}|d_\alpha(\mathbf{a}_s^{\mathrm{cc}})|\tilde{\psi}_t^{(j)}\rangle\langle\tilde{\psi}_t^{(j)}|d_\beta(\mathbf{a}_s^{\mathrm{cc}})|\tilde{\psi}_s^{(0)}\rangle}{(\omega_{t,j}-\omega_{s,0})} \\
&= \sum_{s\in U}\alpha_{\alpha\beta}^{s} \qquad (7)\\
\alpha_{\alpha\beta}^{U,v} &= f_{\mathrm{occ}}\frac{2}{\hbar}\sum_{\substack{s\neq t\\ s\in U}}\frac{\langle\tilde{\psi}_s^{(0)}|d_\alpha^v|\tilde{\psi}_t^{(j)}\rangle\langle\tilde{\psi}_s^{(t)}|d_\beta^v|\tilde{\psi}_s^{(0)}\rangle}{(\omega_{s,t}-\omega_{s,0})^3} \\
&= \sum_{s\in U}\alpha_{\alpha\beta}^{s,v} \qquad (8)\\
G'^{U,v}_{\alpha\beta}(\{\mathbf{a}_s^{\mathrm{cc}}\}) &= -f_{\mathrm{occ}}\frac{2}{\hbar}\sum_{\substack{s\neq t\\ s\in U}}\frac{\langle\tilde{\psi}_s^{(0)}|d_\alpha^v|\tilde{\psi}_t^{(j)}\rangle\langle\tilde{\psi}_t^{(j)}|m_\beta(\mathbf{a}_s^{\mathrm{cc}})|\tilde{\psi}_s^{(0)}\rangle}{(\omega_{t,j}-\omega_{s,0})^3} \\
&= \sum_{s\in U}G'^{s,v}_{\alpha\beta}(\{\mathbf{a}_s^{\mathrm{cc}}\}) \qquad (9)\\
A^{U}_{\alpha,\beta\gamma}(\{\mathbf{a}_s^{\mathrm{cc}}\}) &= f_{\mathrm{occ}}\frac{2}{\hbar}\sum_{\substack{s\neq t\\ s\in U}}\frac{\langle\tilde{\psi}_s^{(0)}|d_\alpha(\mathbf{a}_s^{\mathrm{cc}})|\tilde{\psi}_t^{(j)}\rangle\langle\tilde{\psi}_t^{(j)}|\theta_{\beta\gamma}(\mathbf{a}_s^{\mathrm{cc}})|\tilde{\psi}_s^{(0)}\rangle}{\omega_{t,j}-\omega_{s,0}} \\
&= \sum_{s\in U}A^{s}_{\alpha,\beta\gamma}(\{\mathbf{a}_s^{\mathrm{cc}}\}) \qquad (10)
\end{aligned}$$

f_{occ} is the occupation number with values of 1 and 2 in the unrestricted and restricted KS framework, respectively. $\hbar$ is Planck's constant divided by 2π and $(\omega_{t,j}-\omega_{s,0})$ the angular frequency difference corresponding to $|\tilde{\psi}_t^{(j)}\rangle$ and $|\tilde{\psi}_s^{(0)}\rangle$ of the excited and ground state, respectively. $d_\alpha(\mathbf{a}_s^{\mathrm{cc}}) = -er_\alpha(\mathbf{a}_s^{\mathrm{cc}})$ (e: elementary charge) is the α component of the electric dipole moment operator for the electrons in the length representation with center of charge as coordinate origin. The d_α^v components of the electronic part of the electric dipole moment operator in the velocity form are independent of the coordinate origin. The electric-dipole–electric-dipole polarizability tensor $\boldsymbol{\alpha}$ is origin independent for neutral molecules both in the length and velocity form. $m_\alpha(\mathbf{a}_s^{\mathrm{cc}}) = -\frac{e}{2m_e}\epsilon_{\alpha\beta\gamma}r_\beta(\mathbf{a}_s^{\mathrm{cc}})p_\gamma$ (m_e: electron mass; p_γ: γ component of momentum operator) indicates the α component of the magnetic dipole operator and $\theta_{\beta\gamma}(\mathbf{a}_s^{\mathrm{cc}})$ the $\alpha\beta$ component of the electronic part of

the electric quadrupole operator in its traceless form (compare Ref. [45]).

Employing the magnetic dipole moment operator $-\frac{e}{2m_e}\epsilon_{\alpha\beta\gamma}r_\beta(\mathbf{a}_s^{\mathrm{cc}})p_\gamma$ as perturbation Hamiltonian in the DFPT calculation in principle requires additional uncoupled self-consistent field DFPT calculations with the correction Hamiltonians $-\frac{e}{2m_e}\epsilon_{\alpha\beta\gamma}(a_{\beta,t}^{\mathrm{cc}} - a_{\beta,s}^{\mathrm{cc}})p_\gamma$ since this perturbation is orbital dependent [69, 70]. Tests however have shown that this has a negligible contribution to the ROA intensities.

The tensors given in Eqs. (7) – (10) are origin independent in that sense that translation of the molecule of interest does lead to the same ROA tensor values since the centers of charge are also shifted accordingly. Nevertheless, calculating the ROA invariants with said ROA tensors in this distributed origin gauge does not lead to meaningful ROA intensities. The latter can be achieved by a common gauge origin.

Choosing the common gauge origin $\mathbf{R}^{\mathrm{com}}$, the $\mathbf{G}'^{s,v}(\{\mathbf{a}_s^{\mathrm{cc}}\})$ and $\mathbf{A}^s(\{\mathbf{a}_s^{\mathrm{cc}}\})$ tensors are translated to the common gauge origin via

$$\begin{aligned} G'^{s,v}_{\alpha\beta}(\mathbf{R}^{\mathrm{com}}) &= G'^{s,v}_{\alpha\beta}(\{\mathbf{a}_s^{\mathrm{cc}}\}) + \frac{1}{2}\epsilon_{\beta\gamma\delta}(a_{\gamma,s}^{\mathrm{cc}} - R_\gamma^{\mathrm{com}})\alpha^{s,v}_{\alpha\delta} \\ &= G'^{s,v}_{\alpha\beta}(\{\mathbf{a}_s^{\mathrm{cc}}\}) + b^{s,v}_{\alpha\beta}(\{\mathbf{a}_s^{\mathrm{cc}} - \mathbf{R}^{\mathrm{com}}\}) \qquad (11) \\ A^s_{\alpha,\beta\gamma}(\mathbf{R}^{\mathrm{com}}) &= A^s_{\alpha,\beta\gamma}(\{\mathbf{a}_s^{\mathrm{cc}}\}) + \frac{3}{2}(a_{\beta,s}^{\mathrm{cc}} - R_\beta^{\mathrm{com}})\alpha^s_{\alpha\gamma} \\ &\quad + \frac{3}{2}(a_{\gamma,s}^{\mathrm{cc}} - R_\gamma^{\mathrm{com}})\alpha^s_{\alpha\beta} - (a_{\delta,s}^{\mathrm{cc}} - R_\delta^{\mathrm{com}}) - \alpha^s_{\alpha\delta}\delta_{\beta\gamma} \\ &= A^s_{\alpha,\beta\gamma}(\{\mathbf{a}_s^{\mathrm{cc}}\}) + g^s_{\alpha,\beta\gamma}(\{\mathbf{a}_s^{\mathrm{cc}} - \mathbf{R}^{\mathrm{com}}\}). \qquad (12) \end{aligned}$$

Here, we have introduced $\mathbf{b}^{s,v}(\{\mathbf{a}_s^{\mathrm{cc}} - \mathbf{R}^{\mathrm{com}}\})$ and $\mathbf{g}^s(\{\mathbf{a}_s^{\mathrm{cc}} - \mathbf{R}^{\mathrm{com}}\})$. We will refer to their contributions to the ROA intensities as gauge-translating contributions. The ROA intensities arising from $\mathbf{G}'^{s,v}(\{\mathbf{a}_s^{\mathrm{cc}}\})$ and $\mathbf{A}^s(\{\mathbf{a}_s^{\mathrm{cc}}\})$ elements will be denoted as c_{charge}-based contributions in the following. The velocity form of the electric dipole moment operator is used in the evaluation of the $\beta(\mathbf{G}')^2$ invariant, which has been shown to provide origin-independent results [33, 45]. The derivatives of the ROA tensors with respect to normal coordinates and subsequently the ROA invariants are evaluated for computation of ROA

intensities. For instance, the $\beta(\mathbf{G}')^2$ contribution for normal mode Q_k is obtained for the c_{charge}-based contribution of subset U using

$$\frac{1}{2}\sum_{s\in U}\sum_{i}\left[3\left(\frac{\partial R^{\text{mw}}_{i_\gamma}}{Q_k}\right)_0\left(\frac{\partial \alpha^{s,v}_{\alpha\beta}}{\partial R^{\text{mw}}_{i_\gamma}}\right)_0\left(\frac{\partial G'^{s,v}_{\alpha\beta}(\{\mathbf{a}^{\text{cc}}_s\})}{\partial R^{\text{mw}}_{i_\delta}}\right)_0\left(\frac{\partial R^{\text{mw}}_{i_\delta}}{Q_k}\right)_0 - \left(\frac{\partial R^{\text{mw}}_{i_\gamma}}{Q_k}\right)_0\left(\frac{\partial \alpha^{s,v}_{\alpha\alpha}}{\partial R^{\text{mw}}_{i_\gamma}}\right)_0\left(\frac{\partial G'^{s,v}_{\alpha\alpha}(\{\mathbf{a}^{\text{cc}}_s\})}{\partial R^{\text{mw}}_{i_\delta}}\right)_0\left(\frac{\partial R^{\text{mw}}_{i_\delta}}{Q_k}\right)_0\right]. \tag{13}$$

Summation over repeated Greek indices is implied. $\mathbf{R}^{\text{mw}}$ are mass-weighted nuclear coordinates, the index i runs over the number of atoms. In an analogous way, the invariants based on gauge-translating contributions can be calculated.

Using centers of charge and their assignment to e.g. certain atoms or subsets allows the straightforward evaluation of ROA intensities for subsets chosen according to the question of interest. Moreover, contributions can be split into the contribution originating from the LMOs as gauge origins and their translation to the common gauge (or other gauges), respectively.

This approach is different from the one proposed by Hug [49] where the ROA tensors themselves are not split into subset contributions but their derivatives with respect to normal modes. For example, the contribution of subset U to the $\beta(\mathbf{G}')^2$ invariant for normal coordinate Q_k is obtained in this approach using

$$\frac{1}{2}\sum_{i\in U}\left[3\left(\frac{\partial R^{\text{mw}}_{i_\gamma}}{Q_k}\right)_0\left(\frac{\partial \alpha_{\alpha\beta}}{\partial R^{\text{mw}}_{i_\gamma}}\right)_0\left(\frac{\partial G'_{\alpha\beta}(\mathbf{R}^{\text{com}})}{\partial R^{\text{mw}}_{i_\delta}}\right)_0\left(\frac{\partial R^{\text{mw}}_{i_\delta}}{Q_k}\right)_0 - \left(\frac{\partial R^{\text{mw}}_{i_\gamma}}{Q_k}\right)_0\left(\frac{\partial \alpha_{\alpha\alpha}}{\partial R^{\text{mw}}_{i_\gamma}}\right)_0\left(\frac{\partial G'_{\alpha\alpha}(\mathbf{R}^{\text{com}})}{\partial R^{\text{mw}}_{i_\delta}}\right)_0\left(\frac{\partial R^{\text{mw}}_{i_\delta}}{Q_k}\right)_0\right]. \tag{14}$$

Summation over repeated Greek indices is again implied. Here, $\boldsymbol{\alpha}$ and $\mathbf{G}'(\mathbf{R}^{\text{com}})$ tensors are obtained in the usual way for the complete system with a common origin.

3 Computational methodology

The ROA calculation based on localized molecular orbitals has been implemented into the CP2K program package [71], extending our recent implementation for the calculation of ROA spectra [45]. The presented calculations rely on the double-harmonic approximation but the ROA tensors can be straightforwardly computed within an ab initio molecular dynamics framework as well. We employ the Gaussian and plane waves method [72] and Kohn–Sham DFT for the electronic structure with the BP86 exchange–correlation density functional [73, 74]. The latter was successfully used in numerous previous calculations [15, 16, 18, 19, 47, 56, 75–77]. In addition, Goedecker–Teter–Hutter (GTH) pseudopotentials [78–80] in combination with the aug-TZV2P-GTH basis sets were applied. Broadening of the spectra was carried out using a Lorentzian band width with a full width at half maximum height of 15 cm^{-1}.

4 Analysis of tryptophan side chain

Tryptophan is an important molecule for many conformational studies and shows distinct ROA properties. The optimized structure of N-acetyl-(S)-tryptophan-N'-methylamide (**1**), which includes structural features of the protein backbone in addition to the tryptophan side chain [56], is shown in Fig. 1 as well as the corresponding calculated centers of charge. As can easily be seen, the latter can be used to get an impression of the bonding properties and free electron pairs (e.g the oxo of the carbonyl group) in the molecule.

The backscattering ROA spectrum is given in Fig. 2 together with the contributions arising from the distributed gauge, i.e. using the centers of charge as gauge origins, and translation to the common gauge (gauge-translating contributions). We use the origin of the coordinate system as the common gauge. The intensities obtained from translation

Figure 1: Optimized structure of N-acetyl-(S)-tryptophan-N'-methylamide (**1**) and calculated charge centers (in pink).

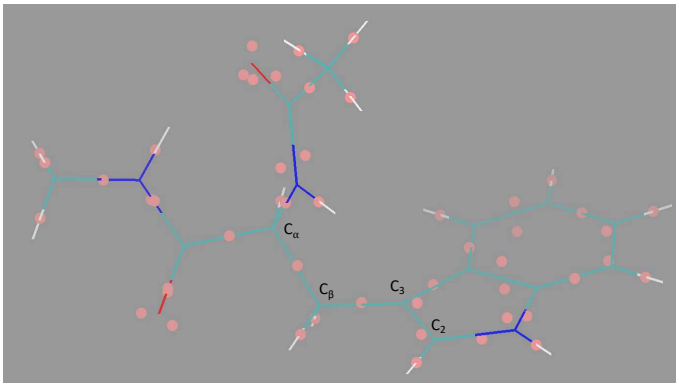

from the distributed to the common gauge origin provide the largest contribution to the overall ROA intensity of most bands. ROA intensities from ROA property tensors with the centers of charge as origin have mainly a significantly smaller contribution (see Fig. 2). Contributions arising from mixed terms (not shown) of gauge-translating and c_{charge}-based contributions play a negligible role for this system.

The strong W3 vibration of the indole ring of tryptophan has been in the focus of various studies. Experiments suggested that the sign of the associated ROA band (experimentally found at around 1550 cm^{-1}) can be used to determine the absolute stereochemistry of a tryptophan side chain [53–55]. Calculations confirmed that the sign of the band is determined by the sign of the ($C_2C_3C_\beta C_\alpha$) torsional angle (see Fig. 1): A positive torsional angle leads to a positive W3 ROA signal whereas a negative angle gives rise to a negative ROA band [56]. A correlation between the magnitude of the ($C_2C_3C_\beta C_\alpha$) torsional angle and the ROA band was not observed in the calculations for (**1**) [56].

The W3 vibration calculated at around 1525 cm^{-1}, which is dominated by a stretching vibration of the indole ring (in particular its five-membered part) and small contributions of a twisting vibration of the $C_\beta H_2$ moiety, is the by far most intense band in Fig. 2. In order to elucidate the origin of its high positive intensity, we have divided (**1**) into three

Figure 2: Backscattering ROA spectra of (**1**): the complete spectrum, the c_{charge}-based contribution resulting from the distributed gauge using centers of charge, and the one arising from the translation of the distributed gauge to the common gauge (gauge-translating contribution).

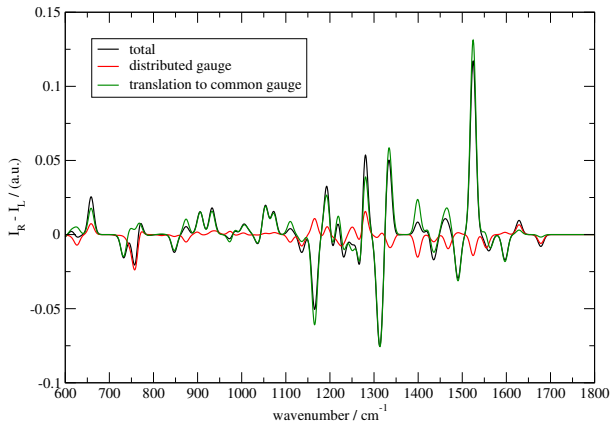

subsets (compare Fig. 3): One subset contains the $C_\beta H_2$ moiety (subset 2) whereas the other subsets contain the indole ring (subset 3) and the remaining part of the molecule (subset 1), respectively. The ROA intensities and invariants according to Eq. (2) were evaluated for each subset using normal mode derivatives. Mixed contributions involving two subsets U and J were generally calculated according to

$$\begin{aligned} \beta(\mathbf{G}')^2_{UJ} &= \frac{1}{4}\left[(3\alpha^U_{\alpha\beta}G'^J_{\alpha\beta} - \alpha^U_{\alpha\alpha}G'^J_{\beta\beta}) + (3\alpha^J_{\alpha\beta}G'^U_{\alpha\beta} - \alpha^J_{\alpha\alpha}G'^U_{\beta\beta})\right] \\ \beta(\mathbf{A})^2_{UJ} &= \frac{1}{4}\left[\alpha^U_{\alpha\beta}\epsilon_{\alpha\gamma\delta}A^J_{\gamma,\delta\beta} + \alpha^J_{\alpha\beta}\epsilon_{\alpha\gamma\delta}A^U_{\gamma,\delta\beta}\right] \end{aligned} \tag{15}$$

where summation about repeated Greek indices is implied.

Analysing the subset ROA intensities calculated for the c_{charge}-based contributions to the W3 band (see Fig. 3), it is obvious that the largest absolute intensity arises from the coupling of subset 1 and 3, though with a negative sign (ca. -0.04 a.u.). The largest

Figure 3: Partitioning of (**1**) into three subsets as well as the ROA backscattering spectra arising from the three subsets; the labels refer to the number of subset(s), "1 and 2", "1 and 3", and "2 and 3" are mixed contributions (for details, see text).

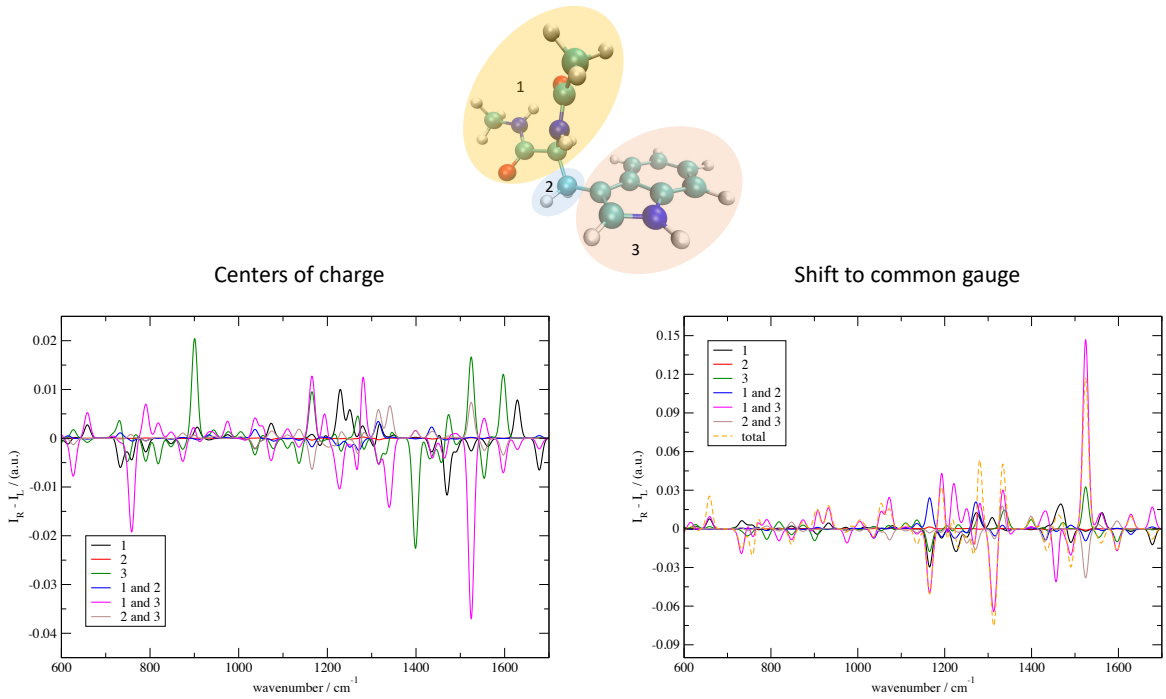

positive intensities for the W3 band are obtained from subset 3 (roughly 0.02 a.u.) and its coupling with subset 2 (approx. 0.01 a.u.). Other contributions are negligibly small. Coming to the gauge-translating contributions, the coupling of subsets 2 and 3 gives now rise to a negative intensity (ca. -0.04 a.u.). This is, however, prevailed by a positive contribution from the coupling between subsets 1 and 3 (approx. 0.15 a.u.), which is by far larger in absolute intensity than the corresponding negative c_{charge}-based contribution. In contrast to that, subset 3 provides again a positive intensity amount (ca. 0.03 a.u.), which is slightly higher than the above-mentioned part emerging from the centers of charge gauge. All in all, the largest part of the final positive ROA intensity of the W3 band comes from the mixed contribution of subsets 1 and 3, which leads in total to a significant positive contribution, and the positive amount resulting from subset 3. The mixing of subsets 2 and 3 leads in total to a minor negative contribution whereas other subsets and mixings thereof have a negligible influence. This demonstrates that the achiral indole moiety plays an essential role for the ROA of the W3 band, which is in accordance with findings using Hug's decomposition analysis [56].

For a more detailed analysis of subset 3, it was divided into four subsets where three are centered on the five-membered ring moiety only and the fourth one consists of the six-membered ring (see Fig. 4). Selected contributions with largest (absolute) intensity for the W3 vibration at ca. 1525 cm^{-1} are given in Fig. 4. The c_{charge}-based contributions are, as already found above, dominated by the indole ring. It becomes clear that its coupling to subset 1, in particular from C_3 (subset 3 in Fig. 4) and the six-membered benzene ring, gives rise to the largest part of the negative ROA intensity observed in Fig. 4. Minor negative contributions (not shown) come from subset 1 and its coupling to subset 5 (NH group) as well. The largest positive contributions originate from coupling within the indole moiety, in particular from the NH group with C_3 and the six-membered ring, respectively. The c_{charge}-based contributions are, nevertheless, small compared to the larger (mainly positive) intensity obtained from the gauge-translating contribution. Especially the large

Figure 4: Division of (**1**) into six subsets as well as the ROA backscattering spectra arising from the six subsets; labels refer to the numbers of subset(s), "and" indicates mixed contributions (for details, see text).

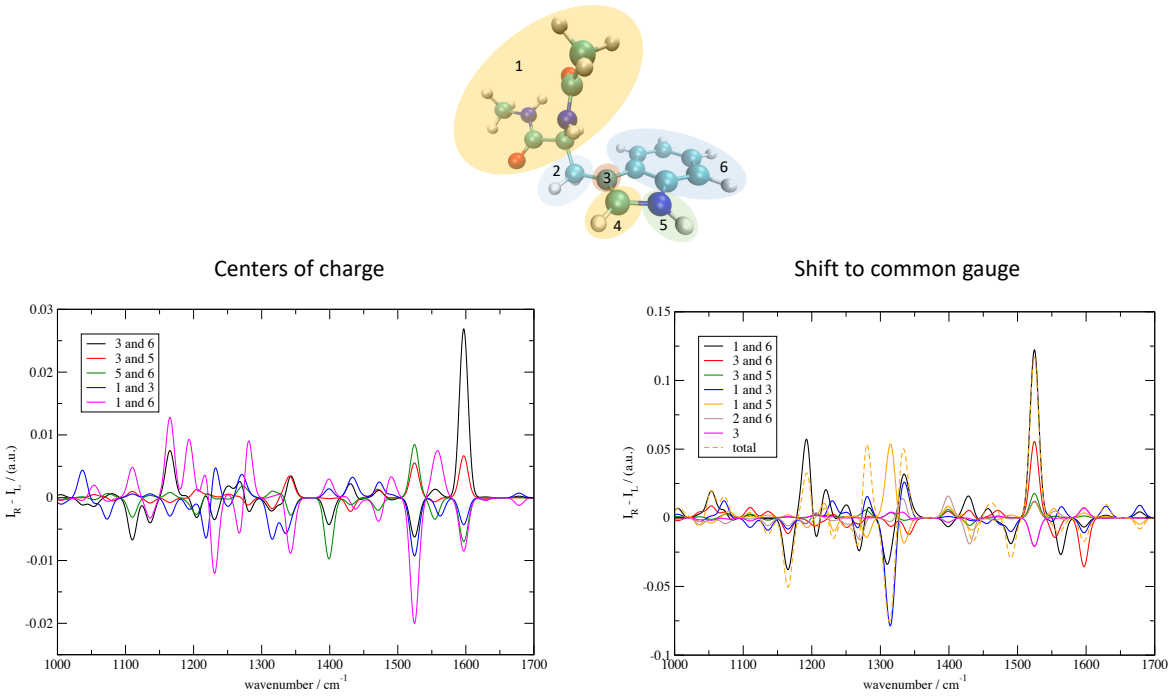

positive amount from the mixed contribution of subsets 1 and 6 (see right-hand side of Fig 4) and, to a smaller amount, from coupling of C_3 and the six-membered ring overall determines the observed strong positive band for the W3 vibration.

In order to explore contributions from subset 1 given in Figs. 3 and 4, we have divided this subset in five subgroups (see Fig. 5): $COCH_3$, NH, CH, CO, and $NHCH_3$. The most intense contributions from this fragmentation are visualized in Fig. 5. The coupling with the indole ring (subset 7 in Fig. 5) is again the dominating part as well as the contribution from subset 7 itself, which gives rise to remarkable positive intensities both for the c_{charge}-based and gauge-translating parts. Mixed contributions from the above-mentioned subgroups with the indole ring lead to negative c_{charge}-based intensities, in particular for subgroup 1 ($COCH_3$) and 2 (NH) (approx. 0.01 a.u.) followed by subgroup 3 (CH) with about 0.008 a.u. and subgroup 4 (CO) providing ca. 0.005 a.u. This is contrary to subset 6 (CH_2), whose c_{charge}-based intensity coming from mixing with the indole ring is positive. Yet, the corresponding gauge-translating intensity is significantly negative so that in total a negative contribution to the W3 band arises for the coupling of subsets 6 and 7. Coupling of the indole ring with other subgroups, as shown in Fig. 5, leads to positive gauge-translating contribution. Especially the mixed contribution from subsets 1 and 7 as well as from 3 and 7 give a significant positive intensity to the final band intensity of more than 0.05 a.u. (and to a smaller amount, coupling of subsets 2 and 7 and also 4 and 7). Subset 5 ($NHCH_3$) obviously plays a negligible role. Adding the c_{charge}-based and gauge-translating intensities, the only negative contribution to the W3-band intensity arises from coupling of the (CH_2) moiety (subset 6) and the indole ring whereas coupling of the latter with other subsets provides overall positive intensities. The highest total positive contribution comes from the indole ring itself.

This makes clear that not necessarily the chiral center and its coupling to other parts of the molecule completely determine the ROA intensity of a band. Instead, an (achiral)

Figure 5: Partitioning of (**1**) into seven subsets as well as the ROA backscattering spectra arising from this partitioning; the labels refer to the number of subset(s), "and" indicates mixed contributions (for details, see text).

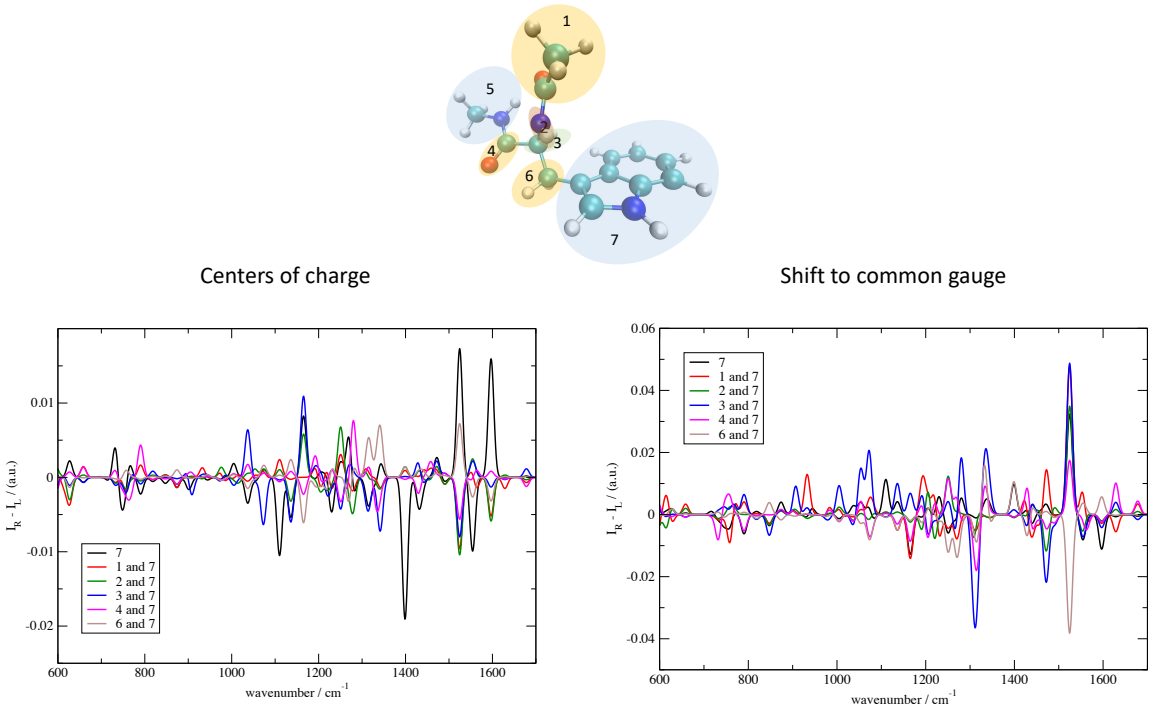

part of a molecule and its couplings to other parts, even if they are not directly adjacent to each other (such as subsets 1 and 7 in Fig. 5), can have a decisive influence.

5 Summary and Outlook

We have presented the first vibrational Raman optical activity calculations based on localized molecular orbitals. Our approach uses computationally efficient density functional perturbation theory for the calculation of the ROA property tensors. Localized molecular orbitals have been obtained utilizing the Foster–Boys criterion and center of charges derived thereof but the approach is not limited to this criterion. It has been demonstrated

that a distributed gauge using the centers of charge as origins is not sufficient to obtain meaningful ROA intensities but translation to a common gauge overcomes this issue. Investigation of the contributions arising from the centers of charge and translation to a common gauge for a tryptophan side chain model has shown that the latter provide the dominating intensity contributions whereas the former lead to remarkably lower absolute intensities for most bands in the spectrum.

The localization of orbitals allows in a straightforward way to divide the compound of interest into subsets, for which contributions to the total observed ROA intensities can be calculated. This approach allows an *a priori* fragmentation of the ROA property tensors, which is different from previously proposed analysis techniques based on partitioning of derivatives with respect to nuclear coordinates belonging to specific atoms. As an example, we have investigated a model for a tryptophan side chain, in particular its W3 band. Splitting into subset contributions showed that the the strong positive W3 band is largely influenced by the (achiral) indole ring as well as its coupling to other parts of the molecule, in particular not adjacent ones such as the distant $COCH_3$ group. This makes clear that the ROA intensity is not necessarily a very local property determined by the chiral center only.

The described computational approach is an attractive way for novel analysis of Raman optical activity and insight into its origin, contributions arising from local properties such as centers of charge, subsets chosen depending on the question of interest and couplings thereof. This will be especially valuable for large and more involved compounds such as proteins, coordination complexes, and challenging liquids. In addition, this methodology offers an efficient way for calculation of complex systems and may be extended to periodic boundary conditions using maximally localized Wannier functions.

Conflicts of interest

There are no conflicts to declare.

Acknowledgment

Funding by the University of Zurich, the Swiss National Science Foundation (grant no: PP00P2_170667), and the University Research Priority Program "Light to Chemical Energy Conversion" (LightChEC) is gratefully acknowledged. The author thanks the Swiss National Supercomputing Center (project ID: s745 and s788) and the Platform for Advanced Computing in Europe for computing resources.

References

[1] R. A. Mata and H. Werner, *Mol. Phys.*, 2007, **105**, 2753–2761.

[2] M. Sparta and F. Neese, *Chem. Soc. Rev.*, 2014, **43**, 5032–5041.

[3] D. Usvyat, L. Maschio, and M. Schütz, *WIREs Comput. Mol. Sci.*, 2018, **8**, e1357.

[4] G. H. Wannier, *Phys. Rev.*, 1937, **52**, 191–197.

[5] N. Marzari and D. Vanderbilt, *Phys. Rev. B*, 1997, **56**, 12847–12865.

[6] P. J. Stephens, *J. Phys. Chem.*, 1985, **89**, 748–752.

[7] K. Nakanishi, N. Berova, and R. W. Woody, *Circular Dichroism: Principles and Applications*, Wiley-VCH, Weinheim, 2000.

[8] P. W. Atkins and L. D. Barron, *Mol. Phys.*, 1969, **16**, 453–466.

[9] L. D. Barron and A. D. Buckingham, *Mol. Phys.*, 1971, **20**, 1111–1119.

[10] W. Hug, S. Kint, G. Bailey, and J. R. Scherer, *J. Am. Chem. Soc.*, 1975, **97**, 5589–5590.

[11] L. D. Barron, M. P. Boogard, and A. D. Buckingham, *J. Am. Chem. Soc.*, 1973, **95**, 603–605.

[12] J. Šebestík and P. Bouř, *Angew. Chem. Int. Ed.*, 2014, **53**, 9236–9239.

[13] J. Kapitán, L. D. Barron, and L. Hecht, *J. Raman Spectrosc.*, 2015, **46**, 392–399.

[14] P. Oulevey, S. Luber, B. Varnholt, and T. Bürgi, *Angew. Chem. Int. Ed.*, 2016, **55**, 11787–11790.

[15] C. R. Jacob, S. Luber, and M. Reiher, *Chem.-Eur. J.*, 2009, **15**, 13491–13508.

[16] S. Luber and M. Reiher, *J. Phys. Chem. B*, 2010, **114**, 1057–1063.

[17] J. Kessler, J. Kapitán, and P. Bouř, *J. Phys. Chem. Lett.*, 2015, **6**, 3314–3319.

[18] T. Weymuth, M. P. Haag, K. Kiewisch, S. Luber, S. Schenk, C. R. Jacob, C. Herrmann, J. Neugebauer, and M. Reiher, *J. Comput. Chem.*, 2012, **33**, 1165–1175.

[19] S. Luber, *J. Phys. Chem. A*, 2013, **117**, 2760–2770.

[20] S. Yamamoto, *Anal. Bioanal. Chem.*, 2012, **403**, 2203–2212.

[21] S. Yamamoto, J. Kaminsky, and P. Bouř, *Anal. Chem.*, 2012, **84**, 2440–2451.

[22] S. Yamamoto and P. Bouř, *J. Comput. Chem.*, 2013, **34**, 2152–2158.

[23] M. Pecul, A. Rizzo, and J. Leszczynski, *J. Phys. Chem. A*, 2002, **106**, 11008–11016.

[24] S. Luber and M. Reiher, *ChemPhysChem*, 2009, **10**, 2049–2057.

[25] J. R. Cheeseman, M. S. Shaik, P. L. A. Popelier, and E. W. Blanch, *J. Am. Chem. Soc.*, 2011, **133**, 4991–4997.

[26] E. Lamparska, V. Liégeois, O. Quinet, and B. Champagne, *ChemPhysChem*, 2006, **7**, 2366–2376.

[27] J. Drooghaag, J. Marchand-Brynaert, B. Champagne, and V. Liégeois, *J. Phys. Chem. B*, 2010, **114**, 11753–11760.

[28] M. Pecul and K. Ruud, *Int. J. Quantum Chem.*, 2005, **104**, 816–829.

[29] T. D. Crawford, *Theor. Chem. Acc.*, 2006, **115**, 227–245.

[30] K. Ruud and A. J. Thorvaldsen, *Chirality*, 2009, **21**, E54–E67.

[31] L. D. Barron, *Biomed. Spectrosc. Imaging*, 2015, **4**, 223–253.

[32] S. T. Mutter, F. Zielinski, P. L. A. Popelier, and E. W. Blanch, *Analyst*, 2015, **140**, 2944–2956.

[33] S. Luber and M. Reiher, *Chem. Phys.*, 2008, **346**, 212–223.

[34] S. Luber and M. Reiher, *ChemPhysChem*, 2010, **11**, 1876–1887.

[35] C. Johannessen, L. Hecht, and C. Merten, *ChemPhysChem*, 2011, **12**, 1419–1421.

[36] M. Humbert-Droz, P. Oulevey, L. M. Lawson Daku, S. Luber, H. Hagemann, and T. Bürgi, *Phys. Chem. Chem. Phys.*, 2014, **16**, 23260–23273.

[37] S. Luber, *Biomed. Spectrosc. Imaging*, 2015, **4**, 255–268.

[38] K. V. Jovan Jose and K. Raghavachari, *J. Chem. Theory Comput.*, 2016, **12**, 585–594.

[39] T. D. Crawford and K. Ruud, *ChemPhysChem*, 2011, **12**, 3442–3448.

[40] P. Bouř, V. Baumruk, and J. Hanzlikovà, *Collect. Czech. Chem. Commun.*, 1997, **62**, 1384–1395.

[41] V. Liégeois, K. Ruud, and B. Champagne, *J. Chem. Phys.*, 2007, **127**, 204105.

[42] A. J. Thorvaldsen, B. Gao, K. Ruud, M. Fedorovsky, and W. Hug, *Chirality*, 2012, **24**, 1018–1030.

[43] S. Luber, J. Neugebauer, and M. Reiher, *J. Chem. Phys.*, 2009, **130**, 064105.

[44] K. Kiewisch, S. Luber, J. Neugebauer, and M. Reiher, *Chimia*, 2009, **63**, 270–274.

[45] S. Luber, *J. Chem. Theory Comput.*, 2017, **13**, 1254–1262.

[46] L. Jensen, J. Autschbach, M. Krykunov, and G. C. Schatz, *J. Chem. Phys.*, 2007, **127**, 134101.

[47] S. Luber, J. Neugebauer, and M. Reiher, *J. Chem. Phys.*, 2010, **132**, 044113.

[48] L. N. Vidal, T. Giovannini, and C. Cappelli, *J. Phys. Chem. Lett.*, 2016, **7**, 3585–3590.

[49] W. Hug, *Chem. Phys.*, 2001, **264**, 53–69.

[50] L. A. Nafie and T. H. Walnut, *Chem. Phys. Lett.*, 1977, **49**, 441–446.

[51] T. H. Walnut and L. A. Nafie, *Chem. Soc. Rev.*, 1977, **67**, 1501–1510.

[52] L. A. Nafie and T. B. Freedman, *J. Chem. Phys.*, 1981, **75**, 4847–4851.

[53] E. W. Blanch, L. Hecht, L. A. Day, D. M. Pederson, and L. D. Barron, *J. Am. Chem. Soc.*, 2001, **123**, 4863–4864.

[54] T. Miura, H. Takeuchi, and I. Harada, *J. Raman Spectrosc.*, 1989, **20**, 667–671.

[55] H. Takeuchi, *Biopolymers*, 2003, **72**, 305–317.

[56] C. R. Jacob, S. Luber, and M. Reiher, *ChemPhysChem*, 2008, **9**, 2177–2180.

[57] J. Hudevocá, J. Horníček, M. Buděšínský, S. Šebestík, M. Šafařík, G. Zhang, T. A. Keiderling, and P. Bouř, *ChemPhysChem*, 2012, **13**, 2748–2760.

[58] L. D. Barron, *Molecular Light Scattering and Optical Activity*, Cambridge University Press, Cambridge, 2nd ed., 2004.

[59] D. A. Long, *The Raman Effect: A Unified Treatment of the Theory of Raman Scattering by Molecules*, John Wiley & Sons, New York, 2002.

[60] T. M. Black, P. K. Bose, P. L. Polavarapu, L. D. Barron, and L. Hecht, *J. Am. Chem. Soc.*, 1990, **112**, 1479–1489.

[61] E. B. Wilson, Jr., J. C. Decius, and P. C. Cross, *Molecular Vibrations*, McGraw-Hill, New York, 1955.

[62] S. F. Boys, *Rev. Mod. Phys.*, 1960, **32**, 296–299.

[63] J. M. Foster and S. F. Boys, *Rev. Mod. Phys.*, 1960, **32**, 300–302.

[64] N. Marzari, A. A. Mostofi, J. R. Yates, I. Souza, and D. Vanderbilt, *Rev. Mod. Phys.*, 2012, **84**, 1419–1475.

[65] S. Luber, *J. Chem. Phys.*, 2014, **141**, 234110.

[66] S. Luber, M. Iannuzzi, and J. Hutter, *J. Chem. Phys.*, 2014, **141**, 094503.

[67] M. Maestro and R. Moccia, *Mol. Phys.*, 1975, **29**, 81–96.

[68] J. Autschbach and H. F. King, *J. Chem. Phys.*, 2010, **133**, 044109.

[69] D. Sebastiani and M. Parrinello, *J. Phys. Chem. A*, 2001, **105**, 1951–1958.

[70] V. Weber, M. Iannuzzi, S. Giani, J. Hutter, R. Declerck, and M. Waroquier, *J. Chem. Phys.*, 2009, **131**, 014106.

[71]

[72] J. VandeVondele, M. Krack, F. Mohamed, M. Parrinello, T. Chassaing, and J. Hutter, *Comput. Phys. Commun.*, 2005, **167**, 103–128.

[73] A. D. Becke, *Phys. Rev. A*, 1988, **38**, 3098–3100.

[74] J. P. Perdew, *Phys. Rev. B*, 1986, **33**, 8822–8824.

[75] S. Luber, C. Herrmann, and M. Reiher, *J. Phys. Chem. B*, 2008, **112**, 2218–2232.

[76] C. R. Jacob, S. Luber, and M. Reiher, *J. Phys. Chem. B*, 2009, **113**, 6558–6573.

[77] S. Luber and M. Reiher, *J. Phys. Chem. A*, 2009, **113**, 8268–8277.

[78] S. Goedecker, M. Teter, and J. Hutter, *Phys. Rev. B*, 1996, **54**, 1703–1710.

[79] C. Hartwigsen, S. Goedecker, and J. Hutter, *Phys. Rev. B*, 1998, **58**, 3641–3662.

[80] M. Krack, *Theor. Chem. Acc.*, 2005, **114**, 145–152.

for Table of Contents use only

"Localized molecular orbitals for calculation and analysis of vibrational Raman optical activity" by Sandra Luber